Published in final edited form as:
Biochemistry. 2009 June 16; 48(23): 5074–5082. doi:10.1021/bi900345q.

Two prion variants of Sup35p have in-register parallel β-sheet structures, independent of hydration†

Frank Shewmaker[1], **Dmitry Kryndushkin**[1], **Bo Chen**[2], **Robert Tycko**[2], and **Reed B. Wickner**[1,*]

[1] Laboratory of Biochemistry and Genetics, National Institute of Diabetes Digestive and Kidney Disease, National Institutes of Health, Bethesda, MD 20892-0830

[2] Laboratory of ChemicalPhysics, National Institute of Diabetes Digestive and Kidney Disease, National Institutes of Health, Bethesda, MD 20892-0830

Abstract

The [*PSI*$^+$] prion is a self-propagating amyloid of the Sup35 protein, normally a subunit of the translation termination factor, but impaired in this vital function when in the amyloid form. The Sup35 N, M and C domains are the amino-terminal prion domain, a connecting polar domain and the essential C-terminal domain resembling eukaryotic elongation factor 1alpha, respectively. Different [*PSI*$^+$] isolates (prion variants) may have distinct biological properties, associated with different amyloid structures. Here we use solid state NMR to examine the structure of infectious Sup35NM amyloid fibrils of two prion variants. We find that both variants have an in-register parallel β - sheet structure, both in fully hydrated and in lyophilized form. Moreover, we confirm that some leucine residues in the M domain participate in the in-register parallel β-sheet structure. Transmission of the [*PSI*$^+$] prion by amyloid fibrils of Sup35NM and of the [URE3] prion by amyloid fibrils of recombinant full length Ure2p are similar whether they have been lyophilized or not (wet or dry).

A prion is an infectious protein, able to transmit a disease or trait without any essential nucleic acid. This concept arose from studies of the mammalian transmissible spongiform encephalopathies (TSEs), but there are now six known distinct prions in yeast, [URE3], [*PSI*$^+$], [*PIN*$^+$], [β], [*SWI*$^+$], [MCA], and [*OCT*$^+$], based on self-propagating altered forms of Ure2p, Sup35p, Rnq1p, Prb1p, Swi1p, Mca1p, and Cyc8p, respectively (1–6). Extensive evidence, culminating in transfection by the corresponding amyloid of the recombinant protein, has shown that at least [*PSI*$^+$], [URE3], and [*PIN*$^+$] are based on self-propagating amyloids (7–10). Amyloid is a fibrillar protein aggregate characterized by partial protease resistance, birefringence on staining with Congo Red and a cross-β-sheet structure (11).

The Sup35 protein is a subunit of the translation termination factor that is inactivated by its aggregation as amyloid in cells infected with the [*PSI*$^+$] prion. The diminished levels of Sup35p lead to inefficient translation termination and thus more frequent read-through of premature termination codons, for example, suppressing a nonsense mutation in *ADE2* and allowing adenine biosynthesis. Sup35p includes an N-terminal 123 residue prion domain (N), whose normal function is in mRNA turnover (12), a middle 130 residue charged domain (M), and the

†This work was supported by the Intramural Program of the National Institute of Diabetes Digestive and Kidney Diseases.

*For communication: Phone: 301-496-3452, Fax: 301-402-0240, wickner@helix.nih.gov, Bldg. 8, Room 225, NIH, 8 Center Drive MSC 0830, Bethesda, MD 20892-0830.

Supporting Information Available: Supplementary Fig. 1 shows the PITHIRDS-CT data uncorrected for signal from natural abundance ^{13}C. This material is available free of charge via the Internet at http://pubs.acs.org.

C-terminal 432 residue translation termination domain (13–16). The N domain is both necessary and sufficient for prion propagation (14).

A single prion protein sequence can determine several biologically distinguishable infectious entities. In mice, over a dozen TSE variants are recognized, distinguished by incubation period, distribution of pathology in the brain, species barriers, protease sensitivity of PrP^{Sc} and glycoform ratios (reviewed in refs. (17,18)). Variants of the yeast prions [*PSI*$^+$], [URE3] and [*PIN*$^+$] have also been found, distinguished by intensity of the prion phenotype, stability of prion propagation, response to excess or deficiency of some chaperones and ability to cross species barriers (9,19–25). Prion variants are a consequence of different amyloid structures which are faithfully propagated (26,27)

Solid state NMR has been used to study amyloid structure (reviewed in (28)) and different amyloids have been found with in-register parallel β-sheet(29–32), antiparallel β-sheet (33, 34) and parallel β-helix-like (35,36) structures. Solid state NMR structural studies of infectious amyloid of Sup35NM, $Ure2^{1–89}$ and $Rnq1^{153–405}$ (the prion domains) have indicated that each is an in-register parallel β-sheet, meaning that adjacent peptide chains line up in the same N to C orientation, and with corresponding residues opposite each other (Fig. 1) (37–39). The β-sheets are folded along the fibril axis as shown by the diameter of fibrils of the prion domain. Mass per unit length measurements for Ure2p and Sup35p are also consistent with this structure, with each molecule contributing one layer to the fibril (one monomer per 4.7 angstroms fibril length) (40,41). The material used in the solid state NMR studies (37–39) was prepared in a manner known to produce a mixture of prion variants on transfection into yeast cells (8–10). Although this was interpreted to mean that the in-register parallel structure is shared by different variants, it is clearly important to verify that this is the case by direct experiments. Weissman's group has found that cells infected with Sup35NM fibrils produced at 4°C are mostly of a strong variant while those made at 37°C are nearly all a weak variant (8). The 37°C fibrils are more resistant to heat denaturation and breakage and show slow H-D exchange extending further toward the C-terminal part of the prion domain than do fibrils made at 4°C (27). Here we prepare 37°C and 4°C fibrils, verify the expected phenotypes of their transfectants and show that both have in-register parallel β-sheet structure.

NMR experiments require relatively large amounts of material packed into a small volume. Lyophilized fibrils are routinely used for this purpose, and previous solid state NMR studies have shown that lyophilization does not perturb the molecular structures of β-amyloid (34, 42) and HETs(218–289) fibrils (38). Nonetheless, particularly in light of a previous report that hydrated and lyophilized Sup35NM fibrils may have different x-ray diffraction patterns (43), it is important to verify that drying does not perturb the Sup35NM fibril structure. We have therefore analyzed fibrils which have never been dried and find that never-dried fibrils are also in parallel β-sheet structure. Importantly, drying does not produce a difference in infectivity for yeast of either Sup35NM or Ure2p fibrils.

EXPERIMENTAL PROCEDURES

Protein Expression and Purification

Sup35NM was expressed from pFPS167, which codes residues 1–253 with an additional carboxy-terminal histidine tag (see figure 2A). Freshly-transformed BL21-CodonPlus® (DE3) RIPL cells with pFPS167 were grown in Defined Amino-Acid Medium (DAM) for isotopic labeling using adaptations of established methods (37, 44).

Cells were grown overnight in 50 ml LB medium with 50 μg/ml ampicillin, 34 μg/ml chloramphenicol and 100 μg/ml streptomycin, then harvested and re-suspended into 2 liters DAM with 50 μg/ml ampicillin. One liter DAM contains: 100 ml 10x salts (130g/L

KH_2PO_4, 100g/L K_2HPO_4, 90g/L Na_2HPO_4, 20g/L NH_4Cl), 10 ml 100x trace elements (per/100ml: 0.6g $FeSO_4$, 0.6g $CaCl_2$, 0.12g $MnCl_2$, 0.08g $CoCl_2$, 0.07g $ZnSO_4$, 0.03g $CuCl_2$, .002g H_3BO_3, .025g $(NH_4)_6Mo_7O_{24}$, 0.5g EDTA), 10ml 100x MgSO4 (1M), 12ml 40% (w/v) glucose, 100ml 10x TAU mix (0.3g/L thiamine, 2g/L adenine sulfate, 2g/L uracil), and 70ml AA mix (2g/L each amino acid). The cells were grown in DAM at 37°C with vigorous shaking until they reached $A_{600} \approx 1.0$, harvested by centrifugation at ~8,000 × *g* for 7 minutes, and resuspended in 4 liters pre-warmed DAM with the same amino-acid composition, except the amino acid with the desired label had been substituted for the un-labeled counterpart at a concentration of 0.2 g/L. After 15 min shaking at 37°C, protein expression was induced by adding of 1 mM isopropyl-β-D-thiogalactopyranoside (IPTG). After ~4 hours, the cells were harvested at ~8,000 × *g* and stored at −80°C or taken directly to the first purification step.

Sup35NM was purified as previously described (44). Following protein over-expression, cell pellets were re-suspended in 80ml of 8 M Guanidine, 150 mM NaCl, 100 mM K_2HPO_4, pH8 and incubated at room temperature for about 2 hours. The cell lysate was cleared by high-speed centrifugation (~150,000 × g) for 1 hour. The supernatant was mixed with 6ml nickel-nitrilotriacetic acid agarose (NiNTA from Qiagen) and incubated at 4°C for 1 hour. The sample and NiNTA were poured into a gravity column and washed twice with 10 ml of 8.5 M urea, 100 mM Na_2HPO_4 pH 8, 10 mM Tris pH 8, 150 mM NaCl, 20 mM imidazole and twice with 10 ml of 8.5 M urea, 10 mM Tris pH 7.5, 80 mM NaCl, 20 mM imidazole. The protein was eluted twice with 10 ml of 8.5M urea, 10 mM Tris pH7.5, 80 mM NaCl, 200 mM imidazole.

The eluate from NiNTA was passed through an equilibrated Q Sepharose ion exchange column. Following loading, the column was washed with one column volume of 8.5 M urea, 10 mM Tris pH 7.5, 80 mM NaCl (also used to equilibrate the column). Sup35NM was eluted with an 80 – 160 mM NaCl gradient in the same buffer. The Sup35NM-containing fractions were pooled and dialyzed several times against pre-warmed/cooled 5mM K-PO4, pH7.4, 150mM NaCl using Pierce dialysis cassettes (20,000 molecular weight cut off). Dialysis was always performed at 4°C or 37°C accordingly. Sup35NM samples were incubated at their respective temperatures for at least 1 week.

Fibrils were harvested at by high-speed centrifugation (~150,000 × g), which also served to separate fibrils from remaining soluble contaminants. Fibrils were washed several times with water. To achieve very dense samples for solid state NMR, the fibrils were spun at ~280,000 × *g* for 30 minutes.

Ure2p was expressed from pKT41-1 (40), purified by affinity chromatography, dialyzed against 50 mM sodium phosphate pH 8.0, 300 mM NaCl and fibers formed at room temperature with agitation.

Transfection

Sup35NM fibrils were tested for infectivity by transfection into *Saccharomyces cerevisiae* strain 74-D694 (*MATa ade1–14 ura3 leu2 trp1 his3* [*psi*−](45) and Ure2p fibrils into *S. cerevisiae* strain DK174 (*MATa kar1* P_{DAL5}*ADE2 ura3 trp1 leu2 his3*) as previously described (9,46).

Electron Microscopy

The formation of Sup35NM fibrils was confirmed by electron microscopy of negatively stained samples. Aqueous suspensions of fibrils were dispensed to carbon-coated copper grids and incubated for several minutes. The fibril suspensions were blotted away, the grids were briefly washed with water and then 2% uranyl acetate stain was applied to the grids for ~ 2 minutes.

The stain was blotted away and the grids were left to air dry. Fibrils were visualized using an FEI Morgagni transmission electron microscope operating at 80kV.

Nuclear Magnetic Resonance

Solid state NMR experiments on selectively labeled Sup35NM fibrils were performed at room temperature at 9.39 T (100.4 MHz ^{13}C NMR frequency) using an InfinityPlus spectrometer (Varian, Palo Alto, CA) and MAS spinning probes with 3.2 mm diameter rotors (Varian). ^{13}C NMR spectra were recorded at an MAS frequency of 20 kHz with ^{1}H-^{13}C cross -polarization (47) and two-pulse phase-modulated decoupling (48). PITHIRDS-CT measurements were done at a MAS frequency of 18 or 20 kHz (49), using spin-lock detection for an improved signal-to-noise ratio (50). Each PITHIRDS-CT data point is the result of 1024 or more scans with a 4s recyle delay.

The raw PITHIRDS-CT data, $S_{raw}(t)$, (with $S_{raw}(0) = 100$) were corrected for the 1.1% natural abundance of ^{13}C based on the roughly linear decay of the signal to 70% of the initial value by 76.8 ms with dry unlabeled samples (37). The corrected signal due to the specific label, S_{cor}, was calculated as $S_{cor}(t) = [S_{raw}(t) - f_{na}(100\text{-}0.39t)]/(1\text{-}f_{na})$, where f_{na} is the fraction of the 13C signal due to natural-abundance spins. For dry samples, we assume all natural abundance and specifically labeled residues contribute to the signal. For wet samples we estimate f_{na} assuming that natural abundance carbonyl ^{13}C from all of N and 1/3 of M contribute to the signal. This estimate is based on our finding that part of the M domain is in β-sheet structure and contributes to the signal, but part is not, and is presumed to be unstructured (see Results). If all of M were structured, the natural abundance carbonyl ^{13}C correction would increase by one residue equivalent, implying that more leucines are in an in-register parallel beta sheet structure. Thus this is a conservative assumption. The raw PITHIRDS-CT data are shown in supporting information (Fig. S1). Even in the raw data for leucine-1-^{13}C fibrils, it is clear that a significant fraction of the ^{13}C NMR signal decays on the 35 ms time scale typical of in-register parallel beta-sheets with 5 A° intermolecular ^{13}C-^{13}C distances.

Estimation of Leu residues in in-register parallel β sheet structure

With $N_{0.5}$ = number of Leu-1-^{13}C residues ~0.5 nm from its nearest Leu-1-^{13}C neighbor and therefore presumably having in-register parallel β sheet structure, S_{iso} = signal from isolated residues (as in the natural abundance sample), S′ = observed signal from labeled amyloid, $S_{0.5}$ = simulated signal from linear array of ^{13}C atoms 4.7 angstroms apart, and N_{res} = total Leu residues (8),

$$N_{0.5}=N_{res}(S_{iso} - S')/(S_{iso}-S_{0.5}).$$

That is, the location of the signal between that predicted for 0.5 nm spacing ($S_{0.5}$) and that known for isolated labels (S_{iso}) is assumed proportional to the fraction in these forms. For example, if all residues had the 0.5 nm spacing, then S′ would equal $S_{0.5}$ and $N_{0.5}$ would equal N_{res}. If all labeled residues were isolated, then S′ would equal S_{iso} and $N_{0.5}$ would be zero.

Using values at 40 ms:

S_{iso}	$S_{0.5}$	S′dry	$N_{0.5}$	S′wet	$N_{0.5}$	S′rehydr	$N_{0.5}$
85+/ − 5	23+/ − 5	57+/ − 5	3.6	44	5.3	44	5.3

The increased fraction of Leu-1-^{13}C residues estimated to be within 0.5 nm of their nearest neighbor in wet or rehydrated filaments can be accounted for if ~2.6 residues are mobile in

these preparations and therefore not contributing to the NMR signal. The remaining 1.8 residues are assumed to be structured, but not in in-register parallel β sheets.

2D ^{1}H-^{13}C NMR spectra in Fig. 5 were obtained with MAS at 9.5 kHz. ^{1}H-^{13}C spin polarization transfer between the t_1 and t_2 dimensions was carried out with a refocused INEPT sequence (51), with a total transfer period of 3.4 ms. ^{1}H-^{13}C scalar couplings were refocused in the t_1 dimension by a single ^{13}C π pulse at $t_1/2$, and removed in the t_2 dimension by WALTZ decoupling, with a 7.8125 kHz ^{1}H rf field.

RESULTS

Sup35NM fibrils were prepared as described (8) by incubation at either 4°C or 37°C. Although not clearly distinguishable by electron microscopy (Fig. 2B), the variants produced on transfection into yeast cells were as described, with a strong [*PSI*$^{+}$] variant produced by 4°C fibrils and a weak variant by 37°C fibrils (Fig. 2C).

37°C fibrils and 4°C fibrils both have in-register parallel β-sheet structure

We prepared 4°C and 37°C amyloid fibrils of Sup35NM fully labeled with ^{13}C at the carbonyl position of all tyrosine residues (Fig. 2A), and concentrated them by centrifugation but without drying. The one dimensional spectrum of each (Fig. 3) shows a single carbonyl peak at 172.84 ppm with a full width at half height of ~3ppm (Table 1). The tyrosine carbonyl ^{13}C frequency expected for random coil residues is 174.2, and residues in β sheet conformation are shifted 1–3 ppm to lower values while α - helical residues show shifts to higher values (33,52–54). The tyrosine residues of Sup35NM are distributed throughout the N domain but are absent from the M domain (Fig. 2A); this result indicates that all or nearly all are in β sheet conformation for amyloids of both prion variants.

The rapid molecular motion of proteins in solution averages out dipole-dipole interactions and chemical shift anisotropies (CSA), but in solid state ^{13}C NMR, magic angle spinning (MAS) of the sample is needed to average out dipole-dipole interactions and CSA. Pulse sequences that selectively restore ^{13}C-^{13}C dipole-dipole interactions are useful for measuring nearest neighbor distances because the magnitude of the interaction between ^{13}C-labeled atoms is proportional to $1/r^3$. Such pulse sequences are called “dipolar recoupling” sequences. We used the PITHIRDS-CT sequence(49), which has been shown to be particularly effective in measurements of relatively large ^{13}C-^{13}C distances (> 4 Å), even among ^{13}C-labeled sites with large CSA. In PITHIRDS-CT measurements, a radio-frequency (rf) pulse occupying one third of each MAS rotation period and rotating the spins of interest by π (thus “PITHIRDS”) recouples the dipole-dipole interactions. The effective time of recoupling is varied by shifting certain pulses within the rotation period(49), but with a constant total time before the signal is measured (hence CT = constant time) to minimize effects of T_2 relaxation on the experimental data.

The rate of decay of ^{13}C NMR signals under the PITHIRDS-CT sequence depends on distances among ^{13}C nuclei, as shown by the simulations in Fig. 4. Wet (never dried) fibrils of Sup35NM labeled with Tyr-1-^{13}C and formed at 4°C or at 37°C each show rates of signal decay indicating a 4.5 – 5.0 Å distance to the nearest neighbor (Fig. 4A), indicating an in-register parallel β-sheet structure as previously shown for fibrils formed at 20°C (37).

The Sup35 M domain has partial β sheet structure in both 4°C and 37°C filaments

There are 8 leucine residues in Sup35NM, only one of which is in the N domain (Fig. 2A). Sup35NM leucine-1-^{13}C filaments formed at 4°C or 37°C were examined, without drying, by solid state NMR 1D analysis (Fig. 3, Table 1). The carbonyl peak was best fit by two (or in

one case three) Gaussian peaks. The major peak for both samples, accounting for 58% of the signal (~4.6 residues), has a chemical shift of ~173 ppm which is a frequency typical of β sheet structure.

PITHIRDS-CT experiments on leucine-1-^{13}C filaments, carried out as for tyrosine-1-^{13}C labeled filaments (above), showed less rapid decay, indicating that not all of the leucine residues had the nearest-neighbor ^{13}C-^{13}C distances of approximately 5 Å characteristic of in-register parallel β-sheets. Assuming that the signal is a sum of residues in in-register parallel β-sheets and residues outside the β-sheets, with >9 Å nearest-neighbor distances, the results can be explained if ~3.6 leucines are in the β-sheets. This result, taken with that for the 1D spectra above, suggests ~4 leucine residues are in in-register parallel β-sheets. The filaments formed at 4°C and at 37°C showed nearly the same signal decay rate (Fig. 4B), indicating similar numbers of leucine residues in theβ-sheets in the two samples.

Sup35NM filaments with uniform ^{15}N- and ^{13}C-labeling of leucine residues were also grown at 4°C and 37°C. Two-dimensional (2D) ^{1}H-^{13}C NMR spectra of these samples, obtained at room temperature with measurement conditions appropriate for solution NMR rather than solid state NMR (*i.e.*, ^{1}H-^{13}C polarization transfers mediated by scalar couplings rather than dipole-dipole couplings, and low ^{1}H decoupling powers during detection of ^{13}C NMR signals (55–57)) showed strong crosspeaks at chemical shifts that were within 0.04 ppm and 0.3 ppm (for ^{1}H and ^{13}C, respectively) of random coil values(58) (Fig. 5A). The 2D ^{1}H-^{13}C spectra therefore indicate that a subset of the leucine residues (presumably those leucines that are not involved in β-sheet structure) exist in highly mobile segments of the M domain. 2D spectra of 4°C and 37°C filaments were quite similar, although 37°C filaments showed a more intense minority component in the $^{1}H_{\alpha}/^{13}C_{\alpha}$ crosspeak signal (Fig. 5B).

It was possible that the NMR signals observed under “solution NMR” conditions arose from Sup35NM molecules in solution, rather than from mobile segments of Sup35NM in fibrils. We thus directly compared ^{13}C NMR spectra of Leu-1-13C-labeled Sup35NM fibrils and Tyr-1-^{13}C-labeled Sup35NM fibrils, both as fully hydrated, never dried, centrifuged pellets. Spectra were obtained both with “solution NMR” conditions, i.e., direct pulsing of ^{13}C spins and relatively weak proton decoupling (Fig. 6A and 6B), and with “solid state NMR” conditions, i.e., Hartmann-Hahn cross-polarization of ^{13}C spins and relatively strong proton decoupling (Fig. 6D and 6E). The Leu-labeled sample shows strong, sharp carbonyl ^{13}C signals under solution NMR conditions, while the Tyr-labeled sample shows only weaker, broad carbonyl signals under solution NMR conditions. Both samples show carbonyl ^{13}C signals under solid state NMR conditions, but the signals from the Tyr-labeled sample are stronger. These results support our claim that the mobile Leu residues are from the fibrils themselves, not from free Sup35NM in solutionas the latter possibility would result in mobile Tyr residues as well. In addition, as shown in the figure 6C, we have looked directly for Leu carbonyl signals from free Sup35NM molecules by resuspending and repelleting the fibrils, and then recording a ^{13}C NMR spectrum of the supernatant. We see no signals from free Sup35NM, despite extensive signal averaging. Therefore, we conclude that free Sup35NM does not make a measurable contribution to our NMR measurements.

Dried and never dried samples have similar infectivity for yeast

In order to address the possibility that drying of protein samples may cause irreversible damage to the structure of amyloid fibrils, we compared the infectivity rates for fibrils with and without drying. In this functional assay amyloid fibrils were mixed with plasmid DNA and used to transform non-prion yeast cells by a procedure similar to DNA transformation (8,9). Together with selection for the DNA plasmid, limited adenine in the medium allowed detection of colonies with a prion induced by the fibrils. In these experiments, freshly formed amyloid fibrils were compared with the same fibrils that underwent drying using conditions that were

normally used to prepare samples for solid state NMR experiments. Just before transformation, the dried fibrils were dissolved in water and these re-hydrated fibrils as well as wet (never dried) fibrils were each sonicated. For these experiments we used Sup35NM fibrils formed at 4°C as well as full length Ure2p fibrils formed at room temperature. The result shown in Table 2 clearly indicates that the infectivity rates of dry and wet fibrils are similar for both proteins, so we conclude that drying of amyloid fibrils before the NMR experiments does not cause an irreversible alteration of their biological effects, consistent with prior evidence that lyophilization does not alter the molecular structures of amyloid fibrils significantly (*i.e.*, NMR chemical shifts of lyophilized and fully hydrated fibrils are the same(34,38,42)).

Solid state NMR of dried and never dried fibrils

We compared Sup35NM Tyr-1-^{13}C fibrils made at 37°C that had been either dried by lyophilization, as in our previous report (37), or had never been dried (Fig. 4C). The wet fibrils showed, if anything, a more rapid decay of signal in the PITHIRDS-CT experiment, showing that the in-register parallel structure is not a consequence of drying. The one-dimensional solid state NMR spectrum of wet 37°C or 4°C fibrils each showed a single peak with the shift to lower frequencies indicative of β-sheet structure (Table 1). We previously showed that dry Sup35NM Tyr-1-^{13}C 20C fibrils show a major peak indicatingβ-sheet (91%) and a minor non-β-sheet peak (9%).

Dry Sup35NM Leu-1-^{13}C 37°C fibrils showed slower decay in PITHIRDS-CT experiments than did fibrils to which water had been added (Fig 4D), and the one dimensional spectra showed a higher proportion of β-sheet content. Both results can be explained by loss of some non-β-sheet signal in wet samples; unstructured residues should be mobile in the wet sample and then not contribute to the NMR signal. Note that never dried Sup35NM Leu-1-^{13}C 37°C fibrils (Fig. 4B) show essentially the same kinetics as those which had been dried and rehydrated (Fig. 4D).

DISCUSSION

Prions of yeast or mammals are genes made of protein, in the sense that they carry inherited information and, like genes of DNA or RNA, can even have an array of alleles. The alleles are called “strains” in the mammalian literature and “variants” for yeast prions (to avoid confusion with yeast strains). The molecular basis of prion propagation and prion variants clearly involves self-propagating amyloids differing in structure between variants, but for no variant is the atomic structure yet known. Our earlier work has shown that infectious amyloids of Sup35NM, Ure2p$^{1–89}$, and Rnq1p$^{153–405}$ each have an in-register parallel β-sheet structure(37–39). Mutations in the N domain affect different prion variants in different ways suggesting different regions are involved in the β-sheet structure (59,60). H-D exchange experiments show that fibrils formed at 4°C and 37°C had significantly different distributions of the fastest- and slowest- exchanging components (27), indicating significant differences in structure between variant amyloids. In the H-D exchange experiments, most amino acid residues showed a mixture of exchange faster than one minute and exchange slower than one week, indicating that although 4°C and 37°C fibrils each include infectious particles producing mostly a single prion variant, the amyloids in each case are significantly heterogeneous.

Our earlier experiments used dried Sup35NM and Ure2$^{1–89}$ fibrils which, in principle, might alter their structure or infectivity. Here, we show that wet and dry fibrils have the same infectivity, and that, as previously shown for the dry fibrils, the wet Sup35NM fibrils have an in-register parallel β-sheet structure. Our earlier experiments used infectious fibrils, but those fibrils produced a mixture of prion variants. Here, we prepared fibrils at 4°C and 37°C following Tanaka et al. (8), and similarly found that they produced different variants on

transfection into yeast. We showed that in both cases the N (prion) domain had in-register parallel β-sheet structure based on data with Tyr-1-^{13}C labeled fibrils.

We previously estimated that 6–7 of the 8 Leu residues of Sup35NM fibrils formed at 20°C were in β-sheets, and that all β-sheet Leu residues were in in-register parallel structure (37). This indicated that, unexpectedly, the in-register parallel structure extended into the highly charged M domain. Our present data on wet fibrils formed at 4°C or 37°C yields an estimate of 4 residues in in-register parallel β-sheet, consistent with results of Toyama et al. (27), both confirming that the in-register parallel β-sheet structure extends into the charged M domain which contains 7 of the 8 leucines. The different estimates may reflect the different temperatures of sample preparation, a factor shown to be critical in determining structure (27).

Of course, an important caveat of all studies of infectious amyloids is that although yeast prion amyloids are highly infectious, the particle/infectious unit ratio must be quite high, so that it is always possible that the physical properties of the bulk of the amyloid are not those of the minority infectious fibrils.

Given that different variants have in-register parallel β-sheet structure, what is the nature of the difference? The ~7–10 nm diameter of Sup35NM fibrils is a fraction of the length of the extended 123 residue N domain (~40 nm) implying that the sheet must be folded several times along the fibril axis. We have previously suggested that variants may differ by the location of the folds or the length of the loops. Moreover, the data of King and of Weissman (27,60) suggest that the extent of β-sheet structure differs among variants. Differences in the staggering of β-strands in the multilayered structure are also possible (28).

The most important feature of our finding the in-register parallel β-sheet structure for yeast prions of Sup35p, Ure2p and Rnq1p is that this structure provides a clear explanation for how variant information is inherited (39,61,62). The end of the fibril provides a template guiding the conformation assumed by the new monomer joining the fibril to be the same as the last one. The ‘polar zipper’ bonds of Asn and Gln residues(63–65), possible similar interactions between Ser and Thr residues, and the hydrophobic interactions all favor the in-register parallel structure. Only the repulsion of like-charged residues work against forming this structure, and such residues are few in the prion domains of Sup35p, Ure2p and Rnq1p.

Supplementary Material

Refer to Web version on PubMed Central for supplementary material.

Acknowledgments

We thank Brian Kimble for help with protein purification and our colleagues for critical reading of the manuscript.

Abbreviations

CSA
: chemical shift anisotropy

NMR
: nuclear magnetic resonance

MAS
: magic angle spinning

References

1. Wickner RB. [URE3] as an altered *URE2* protein: evidence for a prion analog in *S. cerevisiae*. Science 1994;264:566–569. [PubMed: 7909170]
2. Derkatch IL, Bradley ME, Hong JY, Liebman SW. Prions affect the appearance of other prions: the story of *[PIN]*. Cell 2001;106:171–182. [PubMed: 11511345]
3. Roberts BT, Wickner RB. A class of prions that propagate via covalent auto-activation. Genes Dev 2003;17:2083–2087. [PubMed: 12923060]
4. Du Z, Park KW, Yu H, Fan Q, Li L. Newly identified prion linked to the chromatin-remodeling factor Swi1 in *Saccharomyces cerevisiae*. Nat Genet 2008;40:460–465. [PubMed: 18362884]
5. Nemecek J, Nakayashiki T, Wickner RB. A prion of yeast metacaspase homolog (Mca1p) detected by a genetic screen. Proc Natl Acad Sci USA in press. 2008
6. Patel BK, Gavin-Smyth J, Liebman SW. The yeast global transcriptional co-repressor protein Cyc8 can propagate as a prion. Nat Cell Biol. 2009epub ahead of print
7. King CY, Diaz-Avalos R. Protein-only transmission of three yeast prion strains. Nature 2004;428:319–323. [PubMed: 15029195]
8. Tanaka M, Chien P, Naber N, Cooke R, Weissman JS. Conformational variations in an infectious protein determine prion strain differences. Nature 2004;428:323–328. [PubMed: 15029196]
9. Brachmann A, Baxa U, Wickner RB. Prion generation *in vitro*: amyloid of Ure2p is infectious. Embo J 2005;24:3082–3092. [PubMed: 16096644]
10. Patel BK, Liebman SW. “Prion proof” for [PIN+]: infection with in vitro-made amyloid aggregates of Rnq1p-(132–405) induces [PIN+]. J Mol Biol 2007;365:773–782. [PubMed: 17097676]
11. Sipe JD. Amyloidosis. Annu Rev Biochem 1992;61:947–975. [PubMed: 1497327]
12. Hosoda N, Kobayashii T, Uchida N, Funakoshi Y, Kikuchi Y, Hoshino S, Katada T. Translation termination factor eRF3 mediates mRNA decay through the regulation of deadenylation. J Biol Chem 2003;278:38287–38291. [PubMed: 12923185]
13. Wilson PG, Culbertson MR. *SUF12* suppressor protein of yeast: a fusion protein related to the EF-1 family of elongation factors. J Mol Biol 1988;199:559–573. [PubMed: 3280807]
14. TerAvanesyan A, Dagkesamanskaya AR, Kushnirov VV, Smirnov VN. The *SUP35* omnipotent suppressor gene is involved in the maintenance of the non-Mendelian determinant [psi+] in the yeast *Saccharomyces cerevisiae*. Genetics 1994;137:671–676. [PubMed: 8088512]
15. Frolova L, LeGoff X, Rasmussen HH, Cheperegin S, Drugeon G, Kress M, Arman I, Haenni A-L, Celis JE, Philippe M, Justesen J, Kisselev L. A highly conserved eukaryotic protein family possessing properties of polypeptide chain release factor. Nature 1994;372:701–703. [PubMed: 7990965]
16. Stansfield I, Jones KM, Kushnirov VV, Dagkesamanskaya AR, Poznyakovski AI, Paushkin SV, Nierras CR, Cox BS, Ter-Avanesyan MD, Tuite MF. The products of the *SUP45* (eRF1) and *SUP35* genes interact to mediate translation termination in *Saccharomyces cerevisiae*. EMBO J 1995;14:4365–4373. [PubMed: 7556078]
17. Bruce ME. Scrapie strain variation and mutation. Br Med Bull 1993;49:822–838. [PubMed: 8137131]
18. Collinge J, Clarke AR. A general model of prion strains and their pathogenicity. Science 2007;318:930–936. [PubMed: 17991853]
19. Derkatch IL, Chernoff YO, Kushnirov VV, Inge-Vechtomov SG, Liebman SW. Genesis and variability of [*PSI*] prion factors in *Saccharomyces cerevisiae*. Genetics 1996;144:1375–1386. [PubMed: 8978027]
20. Schlumpberger M, Prusiner SB, Herskowitz I. Induction of distinct [URE3] yeast prion strains. Mol Cell Biol 2001;21:7035–7046. [PubMed: 11564886]
21. Bradley ME, Edskes HK, Hong JY, Wickner RB, Liebman SW. Interactions among prions and prion “strains” in yeast. Proc Natl Acad Sci U S A 2002;99(Suppl 4):16392–16399. [PubMed: 12149514]
22. Kryndushkin D, Wickner RB. Nucleotide exchange factors for Hsp70s are required for [URE3] prion propagation in *Saccharomyces cerevisiae*. Mol Biol Cell 2007;18:2149–2154. [PubMed: 17392510]
23. Kryndushkin D, Shewmaker F, Wickner RB. Curing of the [URE3] prion by Btn2p, a Batten disease-related protein. EMBO J 2008;27:2725–2735. [PubMed: 18833194]

24. Kushnirov VV, Kryndushkin D, Boguta M, Smirnov VN, Ter-Avanesyan MD. Chaperones that cure yeast artificial [*PSI*$^+$] and their prion-specific effects. Curr Biol 2000;10:1443–1446. [PubMed: 11102806]
25. Edskes HK, McCann LM, Hebert AM, Wickner RB. Prion variants and species barriers among *Saccharomyces* Ure2 proteins. Genetics. 200910.1534/genetics.108.099929published ahead of print
26. Bessen RA, Marsh RF. Distinct PrP properties suggest the molecular basis of strain variation in transmissible mink encephalopathy. J Virol 1994;68:7859–7868. [PubMed: 7966576]
27. Toyama BH, Kelly MJ, Gross JD, Weissman JS. The structural basis of yeast prion strain variants. Nature 2007;449:233–237. [PubMed: 17767153]
28. Tycko R. Molecular structure of amyloid fibrils: insights from solid-state NMR. Quart Revs Biophys 2006;1:1–55.
29. Benzinger TL, Gregory DM, Burkoth TS, Miller-Auer H, Lynn DG, Botto RE, Meredith SC. Propagating structure of Alzheimer's beta-amyloid(10–35) is parallel beta-sheet with residues in exact register. Proc Natl Acad Sci U S A 1998;95:13407–13412. [PubMed: 9811813]
30. Antzutkin ON, Balbach JJ, Leapman RD, Rizzo NW, Reed J, Tycko R. Multiple quantum solid-state NMR indicates a parallel, not antiparallel, organization of beta-sheets in Alzheimer's beta-amyloid fibrils. Proc Natl Acad Sci U S A 2000;97:13045–13050. [PubMed: 11069287]
31. Balbach JJ, Petkova AT, Oyler NA, Antzutkin ON, Gordon DJ, Meredith SC, Tycko R. Supramolecular structure in full-length Alzheimer's beta-amyloid fibrils: Evidence for a parallel beta-sheet organization from solid-state nuclear magnetic resonance. Biophys J 2002;83:1205–1216. [PubMed: 12124300]
32. Jaroniec CP, MacPhee CE, Bajaj VS, McMahon MT, Dobson CM, Griffin RG. High-resolution molecular structure of a peptide in an amyloid fibril determined by magic angle spinning NMR spectroscopy. Proc Natl Acad Sci USA 2004;101:711–716. [PubMed: 14715898]
33. Balbach JJ, Ishii Y, Antzutkin ON, Leapman RD, Rizzo NW, Dyda F, Reed J, Tycko R. Amyloid fibril formation by A beta 16–22, a seven-residue fragment of the Alzheimer's beta-amyloid peptide, and structural characterization by solid state NMR. Biochemistry 2000;39:13748–13759. [PubMed: 11076514]
34. Petkova AT, Buntkowsky G, Dyda F, Leapman RD, Yau WM, Tycko R. Solid state NMR reveals a pH-dependent antiparallel beta-sheet registry in fibrils formed by a beta-amyloid peptide. Journal of Molecular Biology 2004;335:247–260. [PubMed: 14659754]
35. Ritter C, Maddelein ML, Siemer AB, Luhrs T, Ernst M, Meier BH, Saupe SJ, Riek R. Correlation of structural elements and infectivity of the HET-s prion. Nature 2005;435:844–848. [PubMed: 15944710]
36. Wasmer C, Lange A, Van Melckebeke H, Siemer AB, Riek R, Meier BH. Amyloid fibrils of the HET-s(218–279) prion form a beta solenoid with a triangular hydrophobic core. Science 2008;319:1523–1526. [PubMed: 18339938]
37. Shewmaker F, Wickner RB, Tycko R. Amyloid of the prion domain of Sup35p has an in-register parallel β-sheet structure. Proc Natl Acad Sci USA 2006;103:19754–19759. [PubMed: 17170131]
38. Baxa U, Wickner RB, Steven AC, Anderson D, Marekov L, Yau W-M, Tycko R. Characterization of β-sheet structure in Ure2p1–89 yeast prion fibrils by solid state nuclear magnetic resonance. Biochemistry 2007;46:13149–13162. [PubMed: 17953455]
39. Wickner RB, Dyda F, Tycko R. Amyloid of Rnq1p, the basis of the [*PIN*$^+$] prion, has a parallel in-register β-sheet structure. Proc Natl Acad Sci U S A 2008;105:2403–2408. [PubMed: 18268327]
40. Baxa U, Taylor KL, Wall JS, Simon MN, Cheng N, Wickner RB, Steven A. Architecture of Ure2p prion filaments: the N-terminal domain forms a central core fiber. J Biol Chem 2003;278:43717–43727. [PubMed: 12917441]
41. Diaz-Avalos R, King CY, Wall JS, Simon M, Caspar DLD. Strain-specific morphologies of yeast prion amyloids. Proc Natl Acad Sci U S A 2005;102:10165–10170. [PubMed: 16006506]
42. Paravastu AK, Petkova AT, Tycko R. Polymorphic fibril formation by residues 10–40 of the Alzheimer's beta-amyloid polypeptide. Biophys J 2006;90:4618–4629. [PubMed: 16565054]
43. Kishimoto A, Hasegawa K, Suzuki H, Taguchi H, Namba K, Yoshida M. beta-Helix is a likely core structure of yeast prion Sup35 amyloid fibers. Biochem Biophys Res Commun 2004;315:739–745. [PubMed: 14975763]

44. Shewmaker F, Ross ED, Tycko R, Wickner RB. Amyloids of shuffled prion domains that form prions have a parallel in-register β-sheet structure. Biochemistry 2008;47:4000–4007. [PubMed: 18324784]
45. Chernoff YO, Lindquist SL, Ono B-I, Inge-Vechtomov SG, Liebman SW. Role of the chaperone protein Hsp104 in propagation of the yeast prion-like factor [psi^{+}]. Science 1995;268:880–884. [PubMed: 7754373]
46. Brachmann A, Toombs JA, Ross ED. Reporter assay systems for [URE3] detection and analysis. Methods 2006;39:35–42. [PubMed: 16762564]
47. Pines A, Gibby MG, Waugh JS. Proton-Enhanced Nmr of Dilute Spins in Solids. J Chem Phys 1973;59:569–590.
48. Bennett AE, Rienstra CM, Auger M, Lakshmi KV, Griffin RG. Heteronuclear Decoupling in Rotating Solids. J Chem Phys 1995;103:6951–6958.
49. Tycko R. Symmetry-based constant-time homonuclear dipolar recoupling in solid-state NMR. J Chem Phys 2007;126:064506. [PubMed: 17313228]
50. Petkova AT, Tycko R. Sensitivity enhancement in structural measurements by solid state NMR through pulsed spin locking. J Mag Res 2002;155:293–299.
51. Morris GA, Freeman R. Enhancement of nuclear magnetic resonance signals by polarization transfer. J Amer Chem Soc 1979;101:760–762.
52. Wishart DS, Sykes BD, Richards FM. Relationship between nuclear magnetic resonance chemical shift and protein secondary structure. J Mol Biol 1991;222:311–333. [PubMed: 1960729]
53. Petkova AT, Ishii Y, Balbach JJ, Antzutkin ON, Leapman RD, Delaglio F, Tycko R. A structural model for Alzheimer's beta-amyloid fibrils based on experimental constraints from solid state NMR. Proc Natl Acad Sci U S A 2002;99:16742–16747. [PubMed: 12481027]
54. Petkova AT, Leapman RD, Guo Z, Yau WM, Mattson MP, Tycko R. Self-propagating, molecular-level polymorphism in Alzheimer's beta-amyloid fibrils. Science 2005;307:262–265. [PubMed: 15653506]
55. Heise H, Hoyer W, Becker S, Andronesi OC, Riedel D, Baldus M. Molecular-level secondary structure, polymorphism, and dynamics of full-length alpha-synuclein fibrils studied by solid-state NMR. Proc Natl Acad Sci USA 2005;102:15871–15876. [PubMed: 16247008]
56. Andronesi OC, Becker S, Seidel K, Heise H, Young HS, Baldus M. Determination of membrane protein structure and dynamics by magic-angle-spinning solid-state NMR spectroscopy. J Amer Chem Soc 2005;127:12965–12974. [PubMed: 16159291]
57. Siemer AB, Arnold AA, Ritter C, Westfeld T, Ernst M, Riek R, Meier BH. Observation of highly flexible residues in amyloid fibrils of the HET-s prion. J Am Chem Soc 2006;128:13224–13228. [PubMed: 17017802]
58. Wishart DS, Bigam CG, Holm A, Hodges RS, Sykes BD. H-1, C-13 and N-15 Random Coil Nmr Chemical-Shifts of the Common Amino-Acids. 1 Investigations of Nearest-Neighbor Effects. J Biomol NMR 1995;5:67–81. [PubMed: 7881273]
59. King CY. Supporting the structural basis of prion strains: induction and identification of [*PSI*] variants. J Mol Biol 2001;307:1247–1260. [PubMed: 11292339]
60. Chang H-Y, Lin J-Y, Lee H-C, Wang H-L, King C-Y. Strain-specific sequences required for yeast prion [PSI+] propagation. Proc Natl Acad Sci U S A 2008;105:13345–13350. [PubMed: 18757753]
61. Ross ED, Minton AP, Wickner RB. Prion domains: sequences, structures and interactions. Nat Cell Biol 2005;7:1039–1044. [PubMed: 16385730]
62. Wickner RB, Shewmaker F, Kryndushkin D, Edskes HK. Protein inheritance (prions) based on parallel in-register β-sheet amyloid structures. Bioessays 2008;30:955–964. [PubMed: 18798523]
63. Perutz MF, Johnson T, Suzuki M, Finch JT. Glutamine repeats as polar zippers: their possible role in inherited neurodegenerative diseases. Proc Natl Acad Sci USA 1994;91:5355–5358. [PubMed: 8202492]
64. Chan JCC, Oyler NA, Yau W-M, Tycko R. Parallel β-sheets and polar zippers in amyloid fibrils formed by residues 10--39 of the yeast prion protein Ure2p. Biochemistry 2005;44:10669–10680. [PubMed: 16060675]
65. Nelson R, Sawaya MR, Balbirnie M, Madsen AO, Riekel C, Grothe R, Eisenberg D. Structure of the cross-β spine of amyloid-like fibrils. Nature 2005;435:773–778. [PubMed: 15944695]

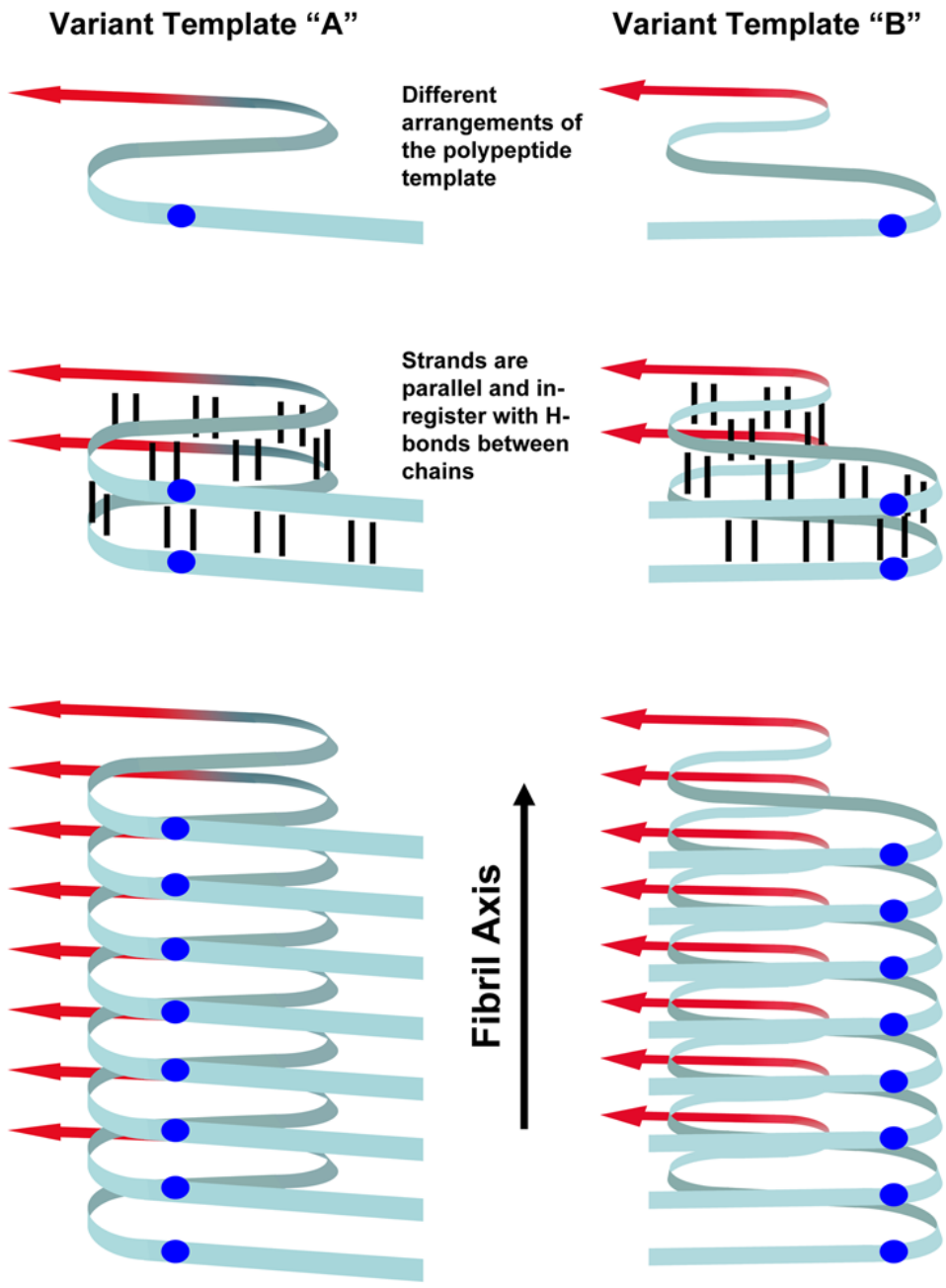

Fig. 1. Model of in-register parallel β-sheet structure

The yeast prions [*PSI*$^{+}$], [URE3] and [*PIN*$^{+}$] are structurally based on in-register parallel β-sheets. The ribbon represents the Prion domain (blue) along with some of the Middle domain (red) of Sup35. The prion conformation is propagated through in-register pairing of the polypeptides thus forming fibrils composed of long parallel β-sheets with the β-strands stacked perpendicularly to the fibril axis. Different prion variants are based on different arrangements of the polypeptide template which are propagated by incorporating free polypeptide into the in-register parallel β-sheets. Residue i of chain n is opposite residue i of the next polypeptide (blue balls) and hydrogen bonds (black lines) to residues i ± 1 of an adjacent chain are parallel to the fibril axis.

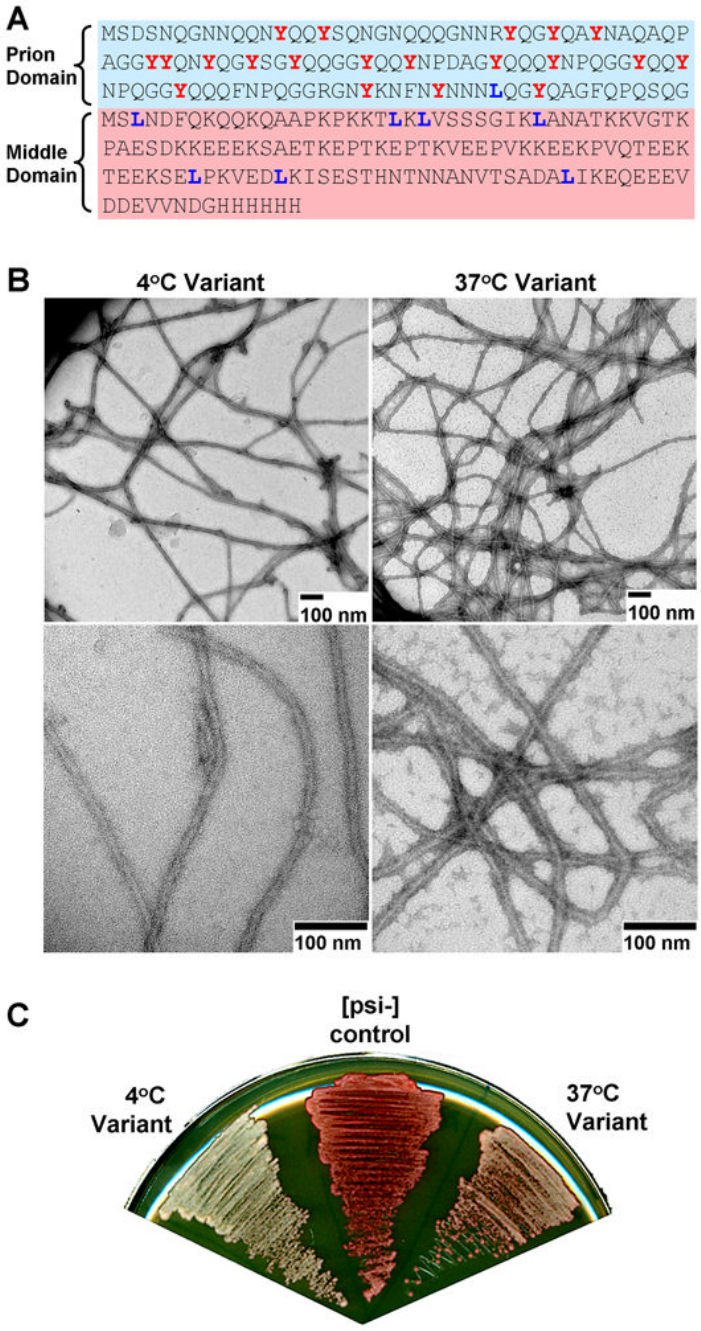

Fig. 2. Sup35NM amyloid fibrils/prions formed at 4° and 37°C

A. All experiments were performed using Sup35NM, which is composed of the prion (N) and middle (M) domain of Sup35, but lacks the C-terminal eRF3 domain. Tyrosine and leucine residues (highlighted in red and blue respectively) were selectively labeled for NMR experiments. B. Following purification in denaturant, Sup35NM was exchanged into phosphate buffer at either 4° or 37°C whereupon it formed long fibrils. C. Fibrils formed at both 4° or 37°C could infect yeast with the [PSI+] prion following transfection. Fibrils grown at 4°C conferred a stronger [PSI+] variant, as reported by whiter yeast colonies on low-adenine medium (see methods).

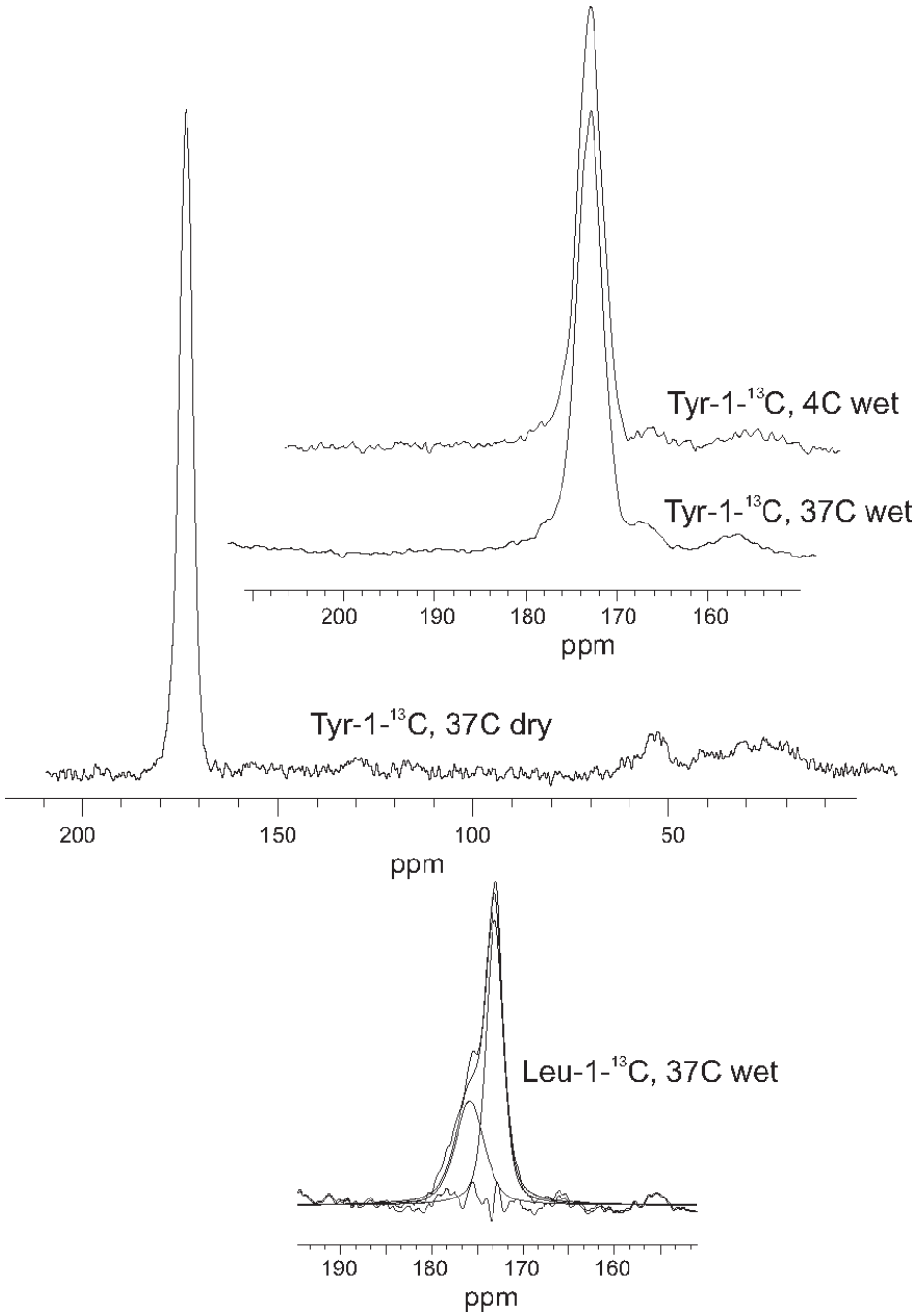

Fig. 3. One dimensional solid state NMR spectra

Spectra of Tyr- and Leu-labeled Sup35NM were recorded at 9.39 T using magic angle spinning at 9.0 kHz. The full spectrum of Tyr-1-^{13}C labeled Sup35NM is shown along with the expanded carbonyl peaks of some of the samples showing the decomposition into major and minor components listed in Table 1.

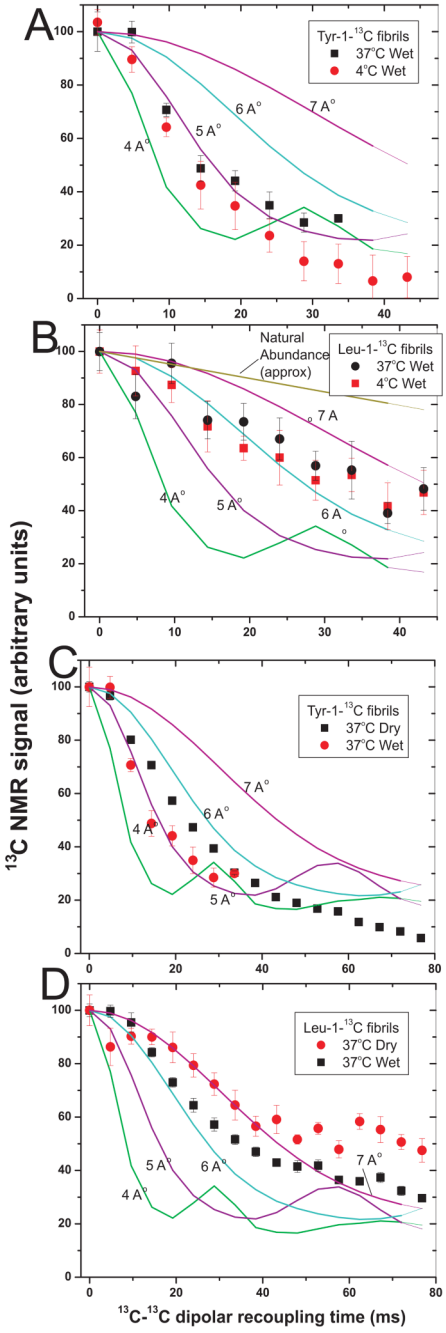

Fig. 4. Dipolar recoupling experiments

Measurements of ^{13}C-^{13}C nuclear magnetic dipole-dipole couplings using the PITHIRDS-CT method at 9.39T. A. Comparison of Tyr-1-^{13}C labeled Sup35NM fibrils formed at 4°C or 37° C using magic angle spinning (MAS) at 18 kHz. Fibrils were compacted by centrifugation, but were never dried. Simulated PITHIRDS-CT curves are shown for ideal linear chains of ^{13}C nuclei with the indicated spacings. B. Comparison of Leu-1-^{13}C labeled Sup35NM fibrils formed at 4°C or 37°C and never dried. C. Comparison of Tyr-1-^{13}C labeled Sup35NM fibrils formed at 37°C and either never dried (wet) or dried by lyophilization (dry). D. Comparison of Leu-1-^{13}C labeled Sup35NM fibrils formed at 37°C and dried by lyophilization (dry) or rehydrated by addition of water (wet).

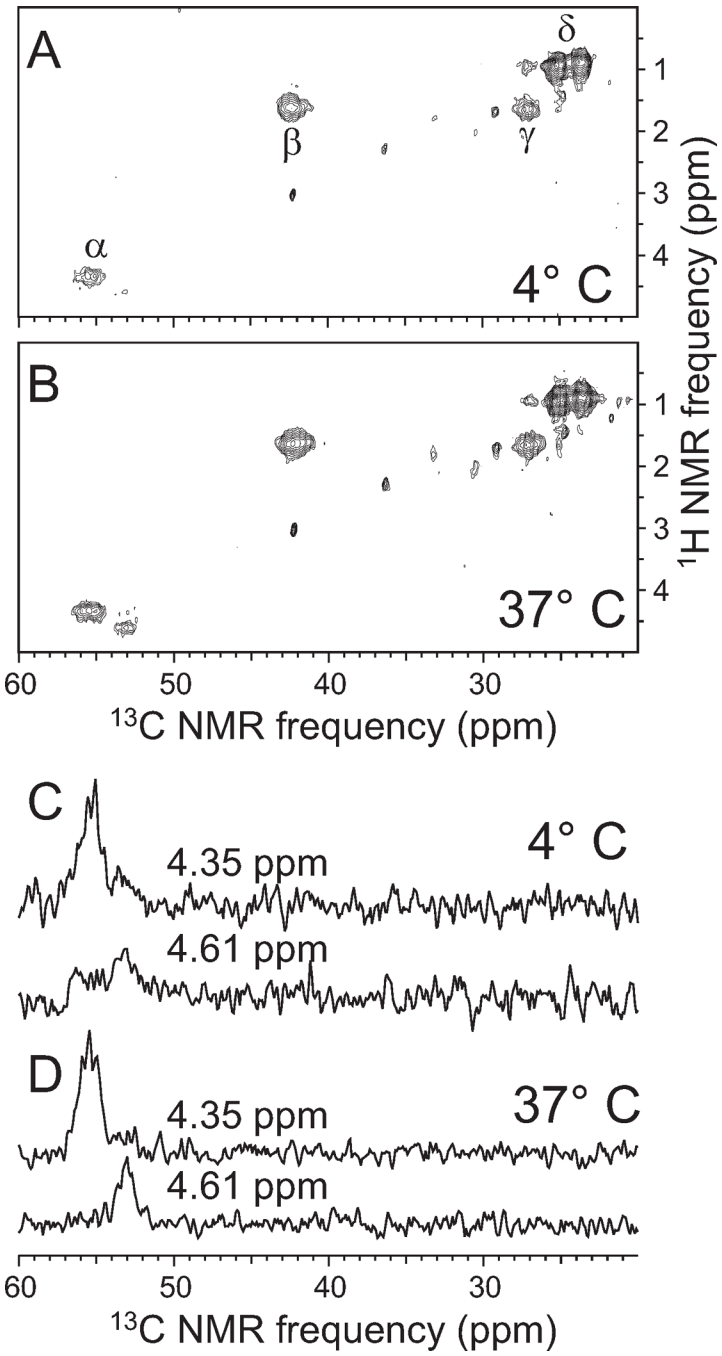

Fig. 5. Two-dimensional ^{1}H-^{13}C NMR spectra

A,B. Spectra of Sup35NM fibrils formed at 4°C and 37°C, with uniform ^{15}N- and ^{13}C-labeling of all leucine residues. Spectra were obtained under conditions appropriate for solution NMR, so that only signals from highly mobile residues are observed. Crosspeaks arising from $^1H_\alpha$/$13C_\alpha$, $^1H_\beta$/$13C_\beta$, $^1H_\gamma$/$13C_\gamma$, and $^1H_\delta$/$13C_\delta$ sites of leucines are indicated. C,D. 1D slices at ^{1}H chemical shifts of 4.35 ppm and 4.61 ppm, corresponding to major and minor components of the $^1H_\alpha$/$13C_\alpha$ signals. The minor component is relatively stronger in the spectrum of 37°C fibrils. Chemical shifts in these spectra are relative to DSS.

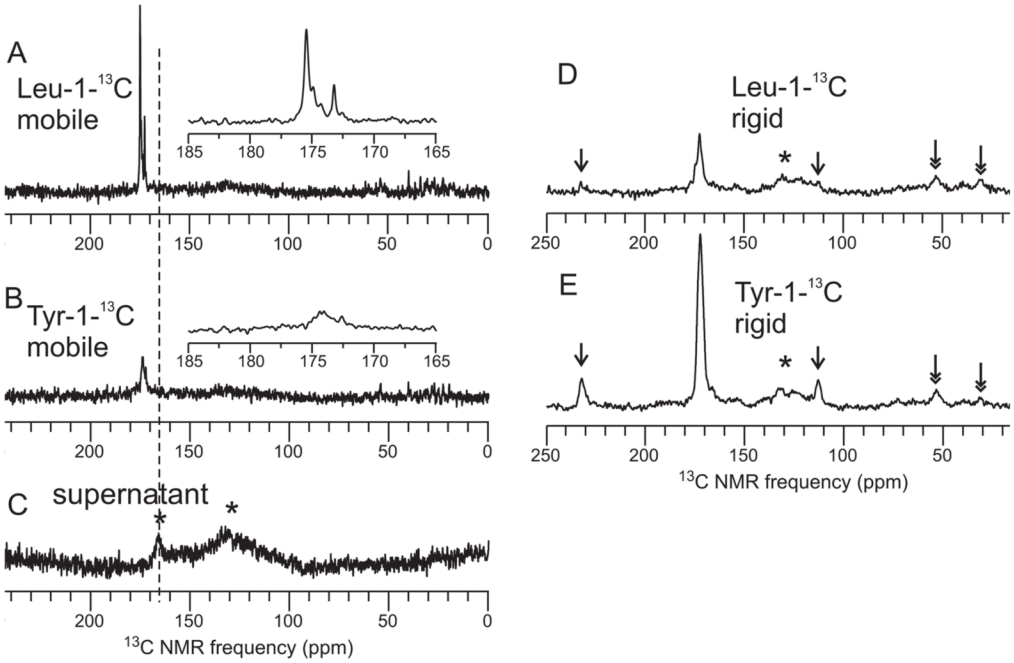

Fig. 6. Comparisons of solution NMR and solid state NMR spectra

A. 1D ^{13}C NMR spectrum of Leu-1-^{13}C labeled Sup35NM fibrils formed at 4° C, obtained with 512 scans under conditions appropriate for observation of highly mobile protein segments, *i.e.*, direct pulsing of ^{13}C, continuous-wave proton decoupling with a 11 kHz rf field, 6.00 kHz MAS frequency, 2.0 s recycle delay. The inset is an expansion of the carbonyl signal region. Sample is a wet pellet (never dried) in a thin-wall 3.2 mm MAS rotor with 36 μl volume, containing 4.6 mg of protein. B. Same as for A, but with 4.9 mg of Tyr-1-^{13}C labeled Sup35NM fibrils formed at 4° C. All sample and measurement conditions are identical, and the vertical scale is the same as in A. C. Same as A, but for the supernatant obtained by suspending the Leu-1-^{13}C labeled Sup35NM fibril pellet in 50 μl H_2O and repelleting. The MAS rotor contains 36 μl of supernatant, 16384 scans were acquired, and the vertical scale is reduced by a factor of four relative to A. Asterisks indicate NMR probe background signals at 130 ppm and 165 ppm. D. Spectrum of Leu-1-^{13}C labeled Sup35NM fibrils formed at 4° C (same sample as in A), obtained with 2048 scans under conditions appropriate for observation of rigid protein segments, *i.e.*, ^{1}H-^{13}C cross-polarization for 1.5 ms, TPPM proton decoupling with an 85 kHz rf field, 6.00 kHz MAS frequency, 2.0 s recycle delay. E. Same as D, but for Tyr-1-^{13}C labeled Sup35NM fibrils formed at 4° C (same sample as in B). Arrows indicate MAS sideband lines, expected from rigid (but not mobile) carbonyl ^{13}C sites due to their chemical shift anisotropy. Double-headed arrows indicate signals from natural-abundance ^{13}C in Sup35NM. Vertical scales in D and E are the same. Nearly equal natural-abundance signal intensities in D and E indicate nearly equal sample quantities.

Table 1

One-dimensional solid state NMR experiments on Sup35NM. The carbonyl peak of each 1D spectrum was fit to a sum of two Gaussian curves. Chemical shifts are relative to tetramethylsilane and random coil shifts are from Wishart et al. (58)

	Major component			Minor components			
label, hydration	**Chemical shift ppm**	**Line width FWHM ppm**	**Fraction**	**Chemical shift ppm**	**Line width FWHM ppm**	**Fraction**	**Random coil ppm**
37°C Leu-1-^{13}C dry	173.24	4	0.88	176.45	2.9	0.12	175.9
37°C Leu-1-^{13}C dry+H_2O	173.29	2.8	0.89	175.8	2.4	0.11	175.9
37°C Leu-1-^{13}C wet	172.61	2.2	0.59	174.93 177.14	2.4 3.1	0.25 0.16	175.9 175.9
4°C Leu-1-^{13}C wet	173.12	2.3	.58	175.36	1.3	.42	175.9
37°C Tyr-1-^{13}C wet	172.84	3.6	1.00				174.2
4°C Tyr-1-^{13}C wet	172.84	3.3	1.0				174.2
37°C Tyr-1-^{13}C dry	172.68	4.3	1.0				174.2

Table 2

Comparison of prion induction by wet and dry amyloid fibrils. Data shown are the average of two experiments. Sup35NM fibrils formed at 4°and Ure2p fibrils formed at room temperature were either used without ever having been dried, or lyophilized to dryness and rehydrated by addition of water. Fibrils were mixed with pRS425 (LEU2) and introduced into spheroplasts selecting plasmid transformants on -Leu with limiting adenine. Over 300 colonies appeared for each fibril type and tests of Ade+ and curability by guanidine showed the indicated fraction of prion-containing transformants. None of the control plasmid transformants without fibrils were Ade+ and curable

protein	Sup35NM	Ure2p	none (control)
final concentration of wet and dry fibrils, μM	1.3	0.8	0
conversion to prion, by wet fibrils (%)	31	22	0
conversion to prion, by dry fibrils (%)	31	20	0